# A Method on Vibration Positioning of Φ-OTDR System Based on Compressed Sensing

Xu Gao, Wenhao Hu, Zhijiang Dou, Kaiwei Li, and Xuepeng Gong

***Abstract*—To improve the accuracy of vibration location information of the Φ-OTDR system, a method of optical fiber sensing signal processing based on Compressed Sensing (CS) is proposed in this paper. First, a sensing matrix is constructed by sparse array and observation array, and the mathematical modeling of CS is established. Then the reconstruction algorithm is designed to complete the accurate reconstruction of the vibration signal with a small number of sampling values. Second, the time domain signal composed of all scattered light at the vibration source is analyzed to complete the measurement of vibration frequency. Finally, a heterodyne Phi-OTDR system is built, using PZT to simulate the vibration source. And 36 scattered light information is continuously collected at the frequency of 100 Hz and 500 Hz. The experimental verification of the CS method in this paper is carried out, besides, the signal-to-noise ratio (SNR) is compared with the traditional difference method, Empirical Mode Decomposition (EMD) method, and Variational Mode Decomposition (VMD) method. The experimental results show that the SNR of this method is improved to 40.41 dB and 30.62 dB, the optimal spatial resolution is 9m, and the maximum relative error of frequency measurement is 8.1%. Compared with the results of traditional I/Q demodulation, the frequency information obtained by the two methods is consistent, and there is no obvious deviation from the actual frequency of PZT. While improving the SNR of the system, this method can greatly simplify the signal processing process and improve the positioning accuracy of the system, which has a certain practical application value in the fields of infrastructure monitoring, resource exploration, and vibration detection.**

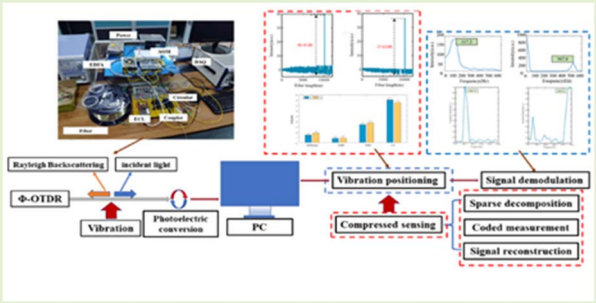


***Index Terms*— Φ-OTDR system, CS, location information, SNR.**

## I. Introduction

SENSOR, as the "five senses" in the field of Instrument Science, undertakes the key task of sensing and obtaining information., which is the source of today's information age.

Manuscript received 8 June 2022; revised 9 July 2022 and 13 July 2022; accepted 13 July 2022. Date of publication 22 July 2022; date of current version 15 August 2022. This work was supported in part by the State Key Laboratory of Applied Optics under Grant SKLAO2021001A03, in part by the Key Research and Development of Jilin Provincial Department of Science and Technology-Key Industrial Core Technology Research Project under Grant 20210201091GX, and in part by the National Natural Science Foundation of China under Grant 62005101. The associate editor coordinating the review of this article and approving it for publication was Prof. Carlos Marques. *(Corresponding author: Xu Gao.)*

Xu Gao is with the School of Opto-Electric Engineering, Changchun University of Science and Technology, Changchun 130022, China, and also with the State Key Laboratory of Applied Optics, Changchun 130022, China (e-mail: gaox19870513@163.com).

Wenhao Hu and Zhijiang Dou are with the School of Opto-electric Engineering, Changchun University of Science and Technology, Changchun 130022, China.

Kaiwei Li is with the Key Laboratory of Bionic Engineering, Ministry of Education, Jilin University, Changchun 130012, China.

Xuepeng Gong is with the State Key Laboratory of Applied Optics, Changchun Institute of Optics, Fine Mechanics and Physics, Chinese Academy of Sciences, Changchun 130033, China.

Digital Object Identifier 10.1109/JSEN.2022.3191863

Optical fiber sensor (OFS) is widely used in electricity, petroleum, chemical industry, construction, environmental protection, military, biomedical, marine observation and so on [1], [2].

OFS is divided into quasi-distribute and distributed [3], [4]. Quasi-distributed fiber optic sensing technology is mainly composed of fiber grating sensing systems, the most representative of which is fiber Bragg grating sensor (FBGS) [5], [6]. When the FBG is under the action of stress or the temperature of its environment changes, the change of its internal parameters will be fully reflected in the change of fiber Bragg wavelength [7], [8]. By detecting the wavelength, we can analyze the changes of the parameters to be measured. Arnaldo G *et al.* form the Federal University of Espírito Santo presented a multiplexing technique for polymer opticalfiber (POF) intensity variation-based sensors. It was also tested in multi-parameter ap-plications, where temperature, angle and force were estimated with errors up to 5% with an array with 3 POF sensors [9]. Distributed optical fiber sensor (DOFS) can obtain the continuous distribution information on the optical fiber, compared with the traditional magnetoelectric sensor, it has the advantages of strong anti-electromagnetic interference ability, corrosion resistance, lightweight, small volume,

long service life, remote monitoring and low maintenance cost [10], [11].

According to different sensing principles, DOFS is divided into interferometric distributed optical fiber sensing technology and scattering distributed optical fiber sensing technology [3], [4]. The phase-sensitive optical time-domain reflectometry (Φ-OTDR) system has unique characteristics in weak signal detection with fast response-ability and high sensitivity [12]. The vibration event of the external environment can be detected by the Φ-OTDR system, which is sensitive to the phase change of backscattered Rayleigh light, including distributed vibration sensor (DVS) and distributed acoustic sensor (DAS) [13]. The former is the intensity change of scattered signal caused by interference effect, which is a qualitative measurement; the latter demodulates the phase change of the scattering signal, which is a quantitative measurement. Qualitative measurement can realize the location of disturbance signal, while the quantitative measurement is to obtain the information of external interference on this basis, and the signal processing methods mainly include denoising and demodulation.

The SNR is an important parameter measuring the performance of the Φ-OTDR system. The environment in which the system is located is often complicated. In addition to the background noise, it also includes the Coherence Rayleigh Noise (CRN) of the Rayleigh Backscattered light (RBS) and the Polarization Relevance Noise (PRN) caused by the birefringence changes of fiber optical fiber. Therefore, researchers are committed to improving the SNR of the system, which is mainly reflected in optimizing the system structure and improving the data processing algorithm.

Bao *et al.* from the University of Ottawa, Canada, used polarization-maintaining fibers to directly improve the quality of the backscattered signal, improving the SNR of the system [14]. Pan *et al.* from the Shanghai Institute of Optics and Mechanics proposed the differential phase-shifting pulse method, which eliminates the influence of coherent fading noise to some extent [15]. The research group of Zhang *et al.* from Nanjing University proposed a structure combining heterodyne detection and a $3 \times 3$ coupler, of which the SNR was 56dB [16]. In the same year, they proposed a method based on orthogonal polarization state pulses to suppress polarization correlation noise, the probe optical pulse pair with orthogonal polarization states is introduced so that the sensitivity of the RBS signal intensity to the polarization state of the probe optical pulse can be eliminated [17]. Shanghai Institute of advanced communication and data science proposed a heterodyne structure using two laser light sources and used the phase difference method to reduce the light source noise, with an average SNR of 37.7db [18]. The methods to improve the SNR by optimizing the system structure are relatively complex, and often require additional components, resulting in high costs. In contrast, the method of suppressing noise by improving the algorithm does not need to change the system structure, which greatly reduces the cost and implementation difficulty. Thus, designing an effective data processing algorithm is an important way to improve the SNR.

Lu *et al.* proposed a method of moving average and moving difference, which processed the collected Rayleigh scattering curves by moving average and moving difference, and finally completed the vibration measurement on a 1.2km fiber, with an SNR of 6.5 dB [19]. Zhu *et al.* proposed a two-dimensional edge detection method for denoising [20]. Yue *et al.* processed the time-domain signals at different positions of the fiber by one-dimensional Fourier transform [21]. Muanenda *et al.* proposed a DMS algorithm, combined with a dual pulse probe, and the SNR of the system reached 24dB [22]. In recent years, with the rapid development of computer and artificial intelligence technology, many scholars have also applied deep learning to the Φ-OTDR system to improve the SNR and reconstruct the signal. Jiang *et al.* used Convolutional Neural Network (CNN) to enhance the signal, the SNR can be increased to 42.8 dB and the signal can be recovered with high fidelity [23]. In 2021, our team proposed the VSS-NLMS method for noise reduction, which improved the positioning accuracy of the Φ-OTDR system [24]. And a new signal processing algorithm is proposed based on this system.

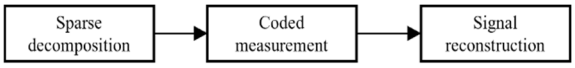


Fig. 1. process of compressed sensing.

For DAS, a method of optical fiber sensing signal processing based on Compressed Sensing (CS) is proposed to improve the SNR. In this article, the mathematical modeling of CS is established. In the actual system, the positioning and demodulation of PZT vibration signals at different frequencies are completed. First, the position of the vibration source is approximated by the differential method, and the accurate position information is further obtained by using the EMD and VMD denoising methods. Then compared with the results of the CS denoising method, the experimental results show that the CS denoising effect is better than other methods, the SNR is increased to 40.41 dB and 30.62 dB, and the positioning accuracy of the system is also improved with simpler signal processing flow and faster data processing speed. Finally, the time-domain signal composed of all scattered light at the vibration source position obtained by the compressed sensing denoising method is subjected to spectrum analysis to obtain the frequency and phase distribution of the PZT vibration signal and compared with the results of I/Q demodulation. As a result, the frequency obtained by the two is similar, but the I/Q demodulation method can obtain the phase information of the vibration signal more accurately.

## II. Compressed Sensing (CS) Method

The process of CS includes three steps: sparse decomposition, coded measurement, and signal reconstruction, whose process is shown in Fig. 1. [25].

The Φ-OTDR system has problems such as a large amount of sensor data and complex noise sources. The signal processing method of the Φ-OTDR system based on CS can effectively remove noise and improve the SNR of the system. In addition, because it is not limited by the sampling theorem, the number of sampling points can be reduced, the data processing speed of the system is optimized to a certain

extent, and the frequency response range of the system is also improved.

First, signal sparsity can be described as that the signal can be approximately represented by a small number of baseline combinations in a certain space. The dimension of the original signal is $n \times 1$. If the non-zero value of the vector is $k$ (k≪n), is named sparsity. It can be linearly expressed on the dimensional sparse transformation basis matrix as:

$$\boldsymbol{x} = \sum_{i=1}^{n} \boldsymbol{\Psi}_i \boldsymbol{s}_i = \boldsymbol{\Psi s} \tag{1}$$

where: $\boldsymbol{s}$ is a vector. $\boldsymbol{\Psi s}$ is the sparse transform basis matrix.

To make the original signal can be represented linearly, most of the commonly used sparse transform matrices are orthogonal matrices, such as orthogonal Fourier transform matrix and partial wavelet transform matrix [26]. Although an orthogonal sparse basis can linearly represent all original signals, not all original signals can be sparsely represented by an orthogonal basis. When the non-zero value of a vector decays exponentially, it can be approximately considered that the vector is sparse in the domain.

Moreover, the key of compressed sensing is not to sparse represent the existing original signal, but to recover the original signal with fewer observations. The observation process of the original signal using the measurement vector can be expressed by the following formula:

$$\boldsymbol{y} = \boldsymbol{\Phi x} = \boldsymbol{\Phi \Psi s} = \boldsymbol{As} \tag{2}$$

where: $\boldsymbol{A}$ is a sensing matrix. $\boldsymbol{\Phi}$ is an observation matrix. $\boldsymbol{\Psi}$ is a sparse matrix.

The equations describe an underdetermined linear system, and the required results are as follows:

1) The solutions of the above equations are obtained;

2) Make the number of non-zero values of the vector as few as possible.

At this point, the problem becomes a problem named $P_0$ [27]. It can be defined as the intersection point of the ball ($l_p^-$) and the solution of equations. While $p \leq 1$, the intersection point tends to fall on the coordinate axis of the ball, and the other coordinates are zero, showing a sparse tendency. The requirements for the matrix include two points: the sparse solution obtained is unique and is the global optimal solution, namely, can be expressed as follows:

$$(P_0) : \min_s \|s\|_0 \quad \text{s.t.} \quad \boldsymbol{As} = \boldsymbol{y} \tag{3}$$

This equation discusses the recovery of the signal in the absence of noise. Therefore, if the matrix $\boldsymbol{A}$ satisfies the Restricted Isometric Property (RIP), the signal reconstruction can be completed by using many reconstruction algorithms.

The characteristics of RIP are required to satisfy the following [28]:

$$(1 - \delta_k) \|\boldsymbol{s}\|_2^2 \leq \|\boldsymbol{As}\|_2^2 \leq (1 + \delta_k) \|\boldsymbol{s}\|_2^2 \tag{4}$$

where: $k$ is the order of the RIP.

Above, it can be seen that it is difficult to prove that the matrix $\boldsymbol{A}$ satisfies the RIP characteristic, but the RIP characteristic can be proved to be irrelevant between the observation matrix and the sparse matrix [29].

Commonly used observation matrices include Gaussian matrix, partial Hadamard measurement matrices, partial orthogonal Fourier transform matrices, random Bernoulli measurement matrices, and sparse random matrices, as well as some constructed cyclic matrices such as Toeplitz matrices.

Tao and Candes proved that the independent identically distributed Gaussian random measurement matrix can become a universal compressed sensing measurement matrix [30]. The advantage of this kind of matrix is that it is not related to most coefficient signals, and the number of measurements required for accurate reconstruction is small. Compared with the deterministic measurement matrix, the Gaussian random matrix can obtain accurate reconstruction with fewer sampling values, and it can be further optimized. In addition, the matrix can be directly generated, and the algorithm design is simpler. Therefore, the Gaussian random matrix is used in this paper.

When the observation matrix $\boldsymbol{\Phi}$ meets the rip condition, the sensing matrix $\boldsymbol{A}$ also probably meets this condition. Each element of the Gaussian matrix, whose order is $m \times n$, obeys the Gaussian distribution, with the mean value of 0 and the variance of *1/M*.

$$\boldsymbol{\Phi}_{i,j} \sim N(0, 1/M) \quad i = 1, 2, \ldots, M \quad j = 1, 2, \ldots, N \tag{5}$$

At last, the Orthogonal Matching Pursuit (OMP) algorithm, which is a kind of greedy algorithm, is used to accurately reconstruct the signal.

The basic idea of the greedy algorithm is to continuously select effective column vectors from the matrix by comparing the correlation between the column vectors of the sensing matrix and the measured values. The criterion for correlation is the inner product of the column vector and the measured value. The limited number of column vectors in the sensing matrix makes the search speed of the greedy algorithm faster. The specific steps of the OMP algorithm are as follows:

1) Input sensing matrix $\boldsymbol{A}$, observation vector $\boldsymbol{y}$, and sparsity $k$.

2) Initialize the residuals and the number of iterations, and select the column vector set.

3) Find the column vector with the largest inner product of the sensing matrix $\boldsymbol{A}$ and residual. And update the index of the selected column vector to the support set, and then update the residual, to complete an iterative process, which is expressed as follows:

$$\boldsymbol{a}_{j\max} = \underset{j=1,2,\ldots,N}{\arg\max} \left\| \boldsymbol{a}_j^T \boldsymbol{r}_0 \right\|_2 \tag{6}$$

$$\boldsymbol{S}_i = \boldsymbol{S}_{i-1} \cup \left\{ \boldsymbol{a}_{j\max} \right\} \tag{7}$$

$$\boldsymbol{r}_i = \boldsymbol{y} - \left( \boldsymbol{S}_i^T \boldsymbol{S}_i \right)^{-1} \boldsymbol{S}_i^T \boldsymbol{y} \tag{8}$$

$$i = i + 1 \tag{9}$$

4) The entire iterative process of step (3) is repeated until the iteration termination condition is satisfied, the number of iterations is equal to the sparsity or the residual is less than a certain set value.

In addition, the reconstruction error is defined to reflect the recovery of each scattered light information, and its specific

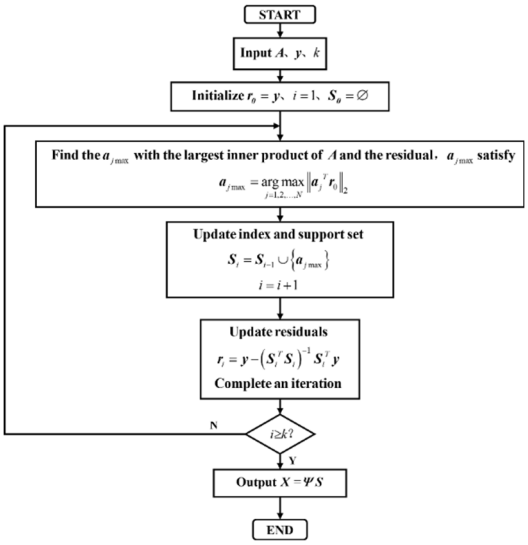


Fig. 2. Flow chart of OMP algorithm.

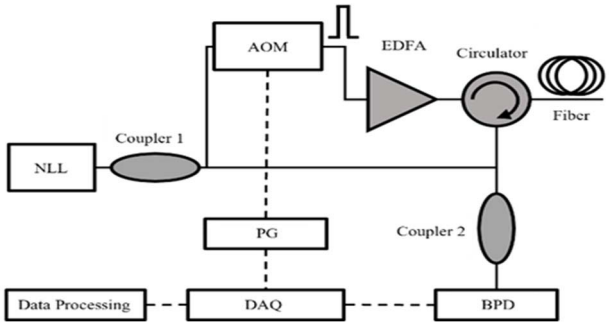


Fig. 3. Heterodyne coherent optical system.

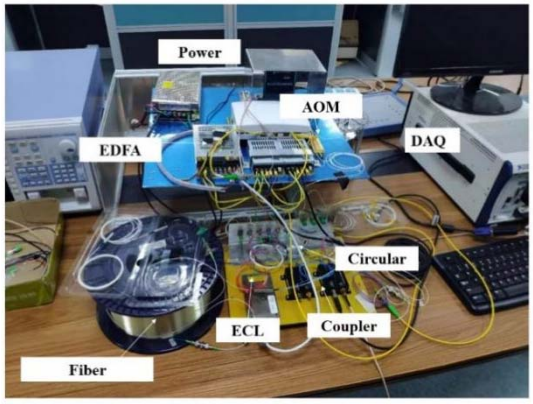


Fig. 4. Experimental platform.

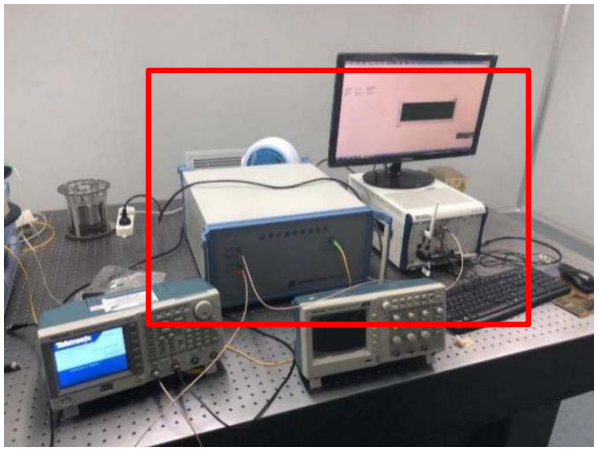

Fig. 5. Experimental platform (Integration).

expression is as follows:

$$\delta = \frac{\|\boldsymbol{s}(z) - \boldsymbol{S}(z)\|_2}{\|\boldsymbol{s}(z)\|_2} \tag{10}$$

where: $\boldsymbol{S}(z)$ is the reconstruction value of scattered light.

The flow chart of the OMP algorithm principle is shown in Fig. 2.

## III. Experiment Part

### A. Φ-OTDR System

The Φ-OTDR system uses the coherence effect between Rayleigh scattered light for sensing and senses external disturbance by detecting its phase change in the fiber. The intensity of the scattered light is used to determine the intrusion location, and the phase of the scattered light is demodulated to obtain intrusion information. Based on the detection principle of the Φ-OTDR system, a heterodyne coherent optical system is shown in Fig. 3. The experimental platform is shown in Fig. 4 and Fig. 5.

The 1550.12nm wavelength is emitted by a narrow linewidth laser (ECL), producing continuous coherent light. Then the continuous wave (CW) is divided into two parts by the 3dB fiber coupler I: 99% signal light and 1% local oscillator light (LO). The signal light enters an Acousto-Optic Modulator (AOM) and is chopped into light pulses with an 80MHz frequency shift. The optical pulse enters an erbium-doped fiber amplifier (EDFA) to amplify the optical power, and then enters the sensing fiber through a four-port circulator, where the sensing fiber is 10.2 km long. The reflected RBS and the local oscillator light are coherent through a 3dB fiber coupler 2 with a splitting ratio of 50:50 to generate a beat frequency signal. The PZT simulated intrusion disturbance signal is loaded into the sensing fiber at a position of 10.14km, and one port of the circulator is connected to a fiber Bragg grating (FBG), which can filter the optical signal. The photo-balanced detector (BPD) receives the optical beat frequency signal and converts it into an electrical signal. At last, the data acquisition card (DAQ) samples the output signal, and it is processed and displayed by the computer. The beat signal collected by the Φ-OTDR system is shown in Eq. (11).

$$I(t) = 2\eta E_{LO}(t) E_b(t) \times \cos(2\pi \Delta f t + \varphi(t) + \varphi_0) \tag{11}$$

where: $\eta$ is the photoelectric conversion coefficient of BPD.

$E_{LO}$ and $E_b$ are the amplitude of local and signal light. $\Delta f$ is the AOM frequency shift. $\varphi(t)$ is the phase change caused by the vibration signal. $\varphi_0$ is the phase change caused by a noise signal.

### B. I/Q Quadrature Demodulation Method

Φ-OTDR obtains the amplitude and phase of backscattered Rayleigh light through I/Q demodulation. The specific steps are as follows:

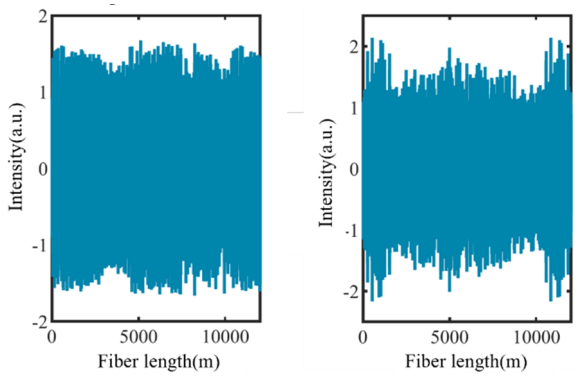


(a)100 Hz (b)500 Hz

Fig. 6. Intensity curve of rayleigh backscattered light.

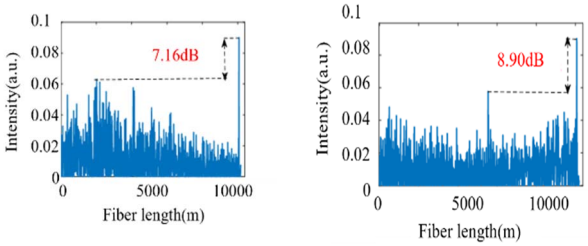


(a) 100 Hz (b) 500 Hz

Fig. 7. Difference denoising results.

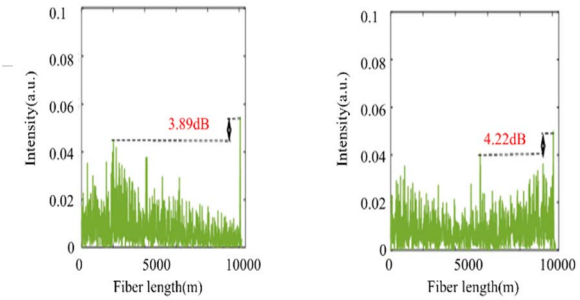


(a) 100 Hz (EMD) (b) 500 Hz (EMD)

Fig. 8. EMD denoising results.

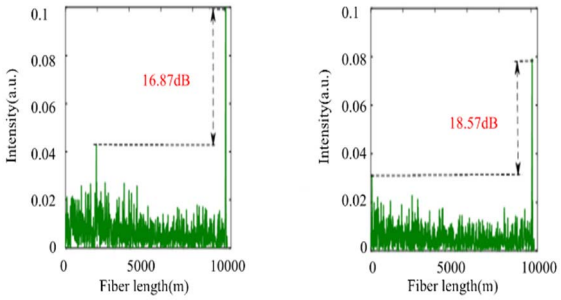


(a) 100 Hz (VMD) (b) 500 Hz (VMD)

Fig. 9. VMD denoising results.

1) A pair of quadrature digital signals with the same frequency was generated as the beat signal. The mathematical equations of the signals are shown in Eq. (12) and Eq. (13).

$$y_{r1} = C\cos\left(2\pi\,\Delta f t + \varphi_r\right) \tag{12}$$

$$y_{r2} = C\cos\left(2\pi\,\Delta f t + \varphi_r\right) \tag{13}$$

where: $C$ is a pair of quadrature signal amplitude. $\varphi_r$ is phase noise.

2) After the multiplied signal is low-pass filtered, a pair of orthogonal signals (I/Q) are acquired in the experiment. The mathematical equations are shown in Eq. (14) and (15).

$$I = E_s\cos\left[\varphi\left(t\right) + \varphi_0 - \varphi_r\right] \tag{14}$$

$$Q = E_s\cos\left[\varphi\left(t\right) + \varphi_0 - \varphi_r\right] \tag{15}$$

where: $E_s$ is the amplitude of quadrature signals I and Q. $\varphi_0 - \varphi_r$ is the phase noise.

3) Finally, the intensity of Rayleigh backscattered light is acquired in Eq. (16).

$$E_s = \sqrt{I^2 + Q^2} \tag{16}$$

### C. Experimental Results and Discussion

During the experiment, PZT applied different frequencies at 10.14km of the optical fiber. Taking 100 Hz and 500 Hz as examples, 36 amplitude curves of Rayleigh backscattered light are collected continuously, and their distribution is shown in Fig.6.

Due to the existence of noise, the position of PZT cannot be obtained directly. Therefore, the method of curve difference between adjacent positions is used to preliminarily locate the vibration source, as shown in Fig.7. The position of the vibration source can be observed by the Difference method, but the SNR is low and the positioning accuracy is not high, so further denoising is needed.

Firstly, this paper adopts the algorithm based on classical empirical mode decomposition (EMD) and variational mode decomposition (VMD) denoising method. The results of 100 Hz and 500 Hz under the EMD denoising method are shown in Fig. 8. And the results under the VMD method are shown in Fig. 9. It can be seen that the denoising effect of VMD is better than that of EMD. However, both methods deal with the results obtained by the Difference method.

Next, the compressed sensing method is applied to the system, aiming at the collected scattered light intensity curve, which doesn't have to deal with the results by the Difference method. So the process is simplified. According to the previous theoretical analysis, the discrete wavelet transform matrix is used as the sparse matrix, the random Gaussian matrix is used as the observation matrix, and the reconstruction algorithm is OMP. The reconstructed results of 36 scattered light with vibration frequencies of 100 Hz and 500 Hz are shown in Fig.10.

The denoising results of the four methods are shown in Fig 11. The SNR obtained by the CS denoising method is significantly higher than that of other methods and has a better denoising effect and higher positioning accuracy. This is mainly caused by the sparse signal itself and non-sparse noise.

At the same time, the CS denoising method in this paper is compared with the VSS-NLMS denoising method proposed by our team. Taking 100 Hz and 500 Hz as examples, the comparison results are shown in Fig. 12.

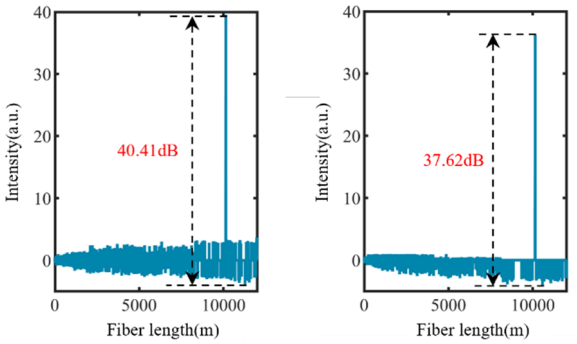


(a)100 Hz (b)500 Hz

Fig. 10. CS denoising results.

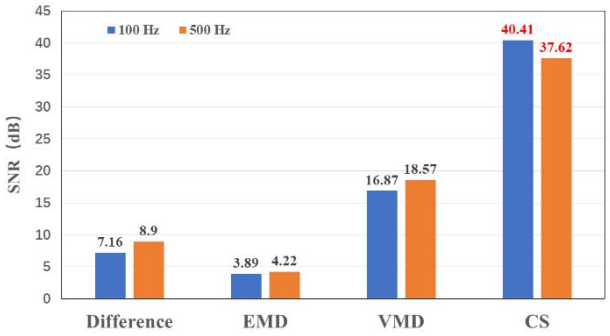


Fig. 11. SNR of four denoising methods.

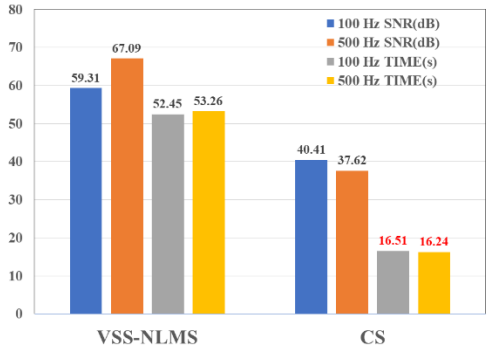


Fig. 12. Comparison results of VSS-NLMS and CS.

It can be seen that although the VSS-NLMS denoising method is better than the CS denoising method in terms of SNR, the CS denoising algorithm greatly reduces the processing time. Similar to EMD and VMD methods, the VSS-NLMS method is also based on the results obtained by the Difference method, and it is necessary to set the expected value for denoising, which is not inconsistent with the actual situation where the frequency of the collected signal is unknown and the standard cannot be set. However, the CS denoising algorithm can denoise the signal directly, which has a small amount of data processing, simpler process, higher efficiency, and better real-time performance, so it can process with a good SNR while collecting at the same time.

As a result, the comparison results of the CS denoising method and other methods are shown in Table I.

In addition, the reconstruction error curves of 36 scattered light is shown in Fig. 13.

TABLE I
COMPARISON RESULTS OF CS AND OTHER METHODS

| | SNR(dB) | | Time(s) | |
|---|---|---|---|---|
| Method | 100 Hz | 500 Hz | 100 Hz | 500 Hz |
| Difference | 7.16 | 8.90 | | |
| EMD | 3.89 | 4.22 | | |
| VMD | 16.87 | 18.57 | | |
| VSS-NLMS | **59.31** | **67.09** | 52.45 | 53.26 |
| CS | **40.41** | **37.62** | **16.51** | **16.24** |

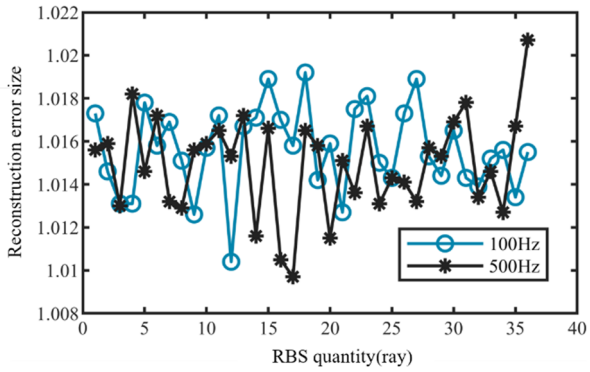


Fig. 13. Scattered light reconstruction error curve.

After locating PZT, the spectrum of 36 scattered light at this position can be obtained, and the actual frequency and phase information at the vibration source frequency of 100 Hz and 500 Hz can be obtained by Fourier transform, as shown in Fig. 14.

To obtain the accurate phase at the vibration source and realize the quantitative measurement of the disturbance signal, the I/Q demodulation method is used for demodulation, the phase demodulation of the I and Q quadrature signals needs to go through three processes of arctangent operation, range expansion, and phase unwrapping. The time domain and frequency domain distributions of the demodulated signal obtained are shown in Fig. 15. It can be seen that the frequency is consistent with the previous results, but the demodulated phase signal is more accurate.

This is because the spectrum analysis of the time-domain signal formed by the collected scattered light at this point is directly carried out after the location of the vibration source is obtained. Due to the influence of noise, phase entanglement, and other factors, the real phase information cannot be obtained.

It should be noted that the results obtained by the compressed sensing denoising method are within an interval, indicating that there is vibration in this range, which is equivalent to its positioning accuracy. To obtain the accurate position of the vibration source to obtain the frequency, the point with the largest amplitude is regarded as the vibration source, and the time-domain signal of the scattered light at the vibration source is constructed according to its coordinate information, which is also one of the error sources of spectrum analysis.

Finally, calculate the spatial resolution and compare it with the theoretical spatial resolution of the experimentally built system. The spatial resolution of the Φ-OTDR system refers

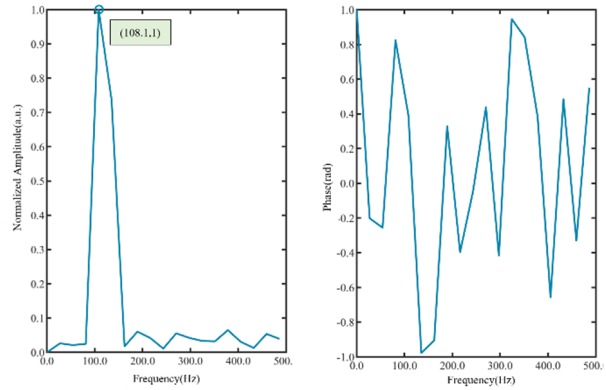


(a) 100 Hz (amplitude) (b) 100 Hz (phase)

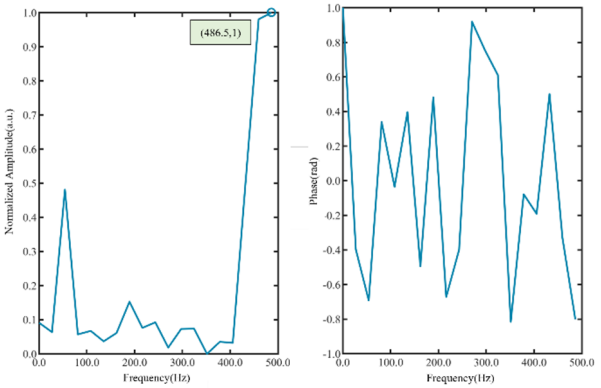


(c) 500 Hz (amplitude) (d) 500 Hz (phase)

Fig. 14. Spectrum analysis results.

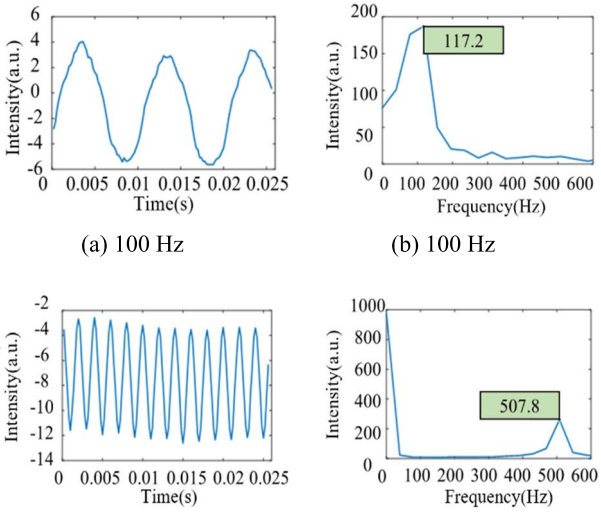


(a) 100 Hz (b) 100 Hz

(c) 500 Hz (d) 500 Hz

Fig. 15. Demodulated signal results.

to the smallest distance between two vibration locations on the sensing fiber. In specific experiments, the length of the sensing fiber corresponding to the curve between 10% and 90% of the scattering power caused by vibration is generally used. When the vibration frequencies of the PZT are 100 Hz and 500 Hz, respectively, the reconstruction results of scattered light are randomly selected for normalization, as shown in Fig. 16.

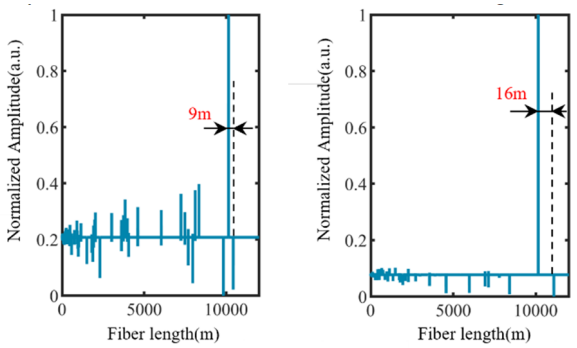


(a)100 Hz (b)500 Hz

Fig. 16. Spatial resolution.

Therefore, it can be obtained that the spatial resolutions of the two frequencies are 9m and 16m respectively, which is close to the theoretical value of 10m. The reason for the difference between the two is not only the influence of noise but also the reconstruction results of each scattered light in the positioning interval are not the same, which brings certain randomness. At the same time, the relative errors of the obtained frequencies are 8.1% and 2.7%. The closer the frequency result is to the PZT simulation value, the more accurate the positioning is.

## IV. Conclusion

In this article, the compressed sensing technology is applied in the Φ-OTDR system and the corresponding signal processing method is designed. The mathematical principle of the CS method is established, and the experiment is designed to verify it. Taking 100 Hz and 500 Hz as an example, the experimental results show that the compressed sensing denoising method can improve SNR to 40.41dB and 30.62 dB respectively at the two frequencies, and the denoising effect is significantly better than the traditional difference method, EMD and VMD denoising methods. As a result, the external interference can be located more accurately, and the signal processing process is simpler. In addition, the spectrum analysis of the time-domain signal at the position of the vibration source is performed and compared with the I/Q demodulation result. The phase information obtained is not good, but the frequency information of the obtained disturbance signal is the same. It shows that this method can not only accurately locate the external intrusion, but also obtain its frequency information, which provides a new idea for the signal processing method of the Φ-OTDR system. Moreover, the signal processing process of this method is simpler, which can save the time of signal processing and more conveniently meet the real-time requirements of the system.

## References

[1] Y. Tong *et al.*, "Development roadmap of optical fiber sensing technology in China," *J. Opt.*, vol. 42, no. 1, pp. 9–42, 2022.

[2] R. Min, Z. Liu, L. Pereira, C. Yang, Q. Sui, and C. Marques, "Optical fiber sensing for marine environment and marine structural health monitoring: A review," *Opt. Laser Technol.*, vol. 140, Aug. 2021, Art. no. 107082.

[3] A. D. Kersey, "A review of recent developments in fiber optic sensor technology," *Opt. Fiber Technol.*, vol. 2, no. 3, pp. 291–317, 1996.

[4] K. T. V. Grattan and T. Sun, "Fiber optic sensor technology: An overview," *Sens. Actuators A, Phys.*, vol. 82, nos. 1–3, pp. 40–61, 2000.
[5] C. Li, J. Tang, C. Cheng, L. Cai, and M. Yang, "FBG arrays for quasi-distributed sensing: A review," *Photonic Sensors*, vol. 11, no. 1, pp. 91–108, Mar. 2021.
[6] A. K. Sharma and C. Marques, "Design and performance perspectives on fiber optic sensors with plasmonic nanostructures and gratings: A review," *IEEE Sensors J.*, vol. 19, no. 17, pp. 7168–7178, Sep. 2019.
[7] G. Meltz, W. W. Morey, and W. H. Glenn, "Formation of Bragg gratings in optical fibers by a transverse holographic method," *Opt. Lett.*, vol. 14, no. 15, pp. 823–825, 1989.
[8] M. Majumder, T. K. Gangopadhyay, A. K. Chakraborty, K. Dasgupta, and D. K. Bhattacharya, "Fibre Bragg gratings in structural health monitoring-present status and applications," *Sens. Actuators A, Phys.*, vol. 147, no. 1, pp. 150–164, 2008.
[9] A. G. Leal-Junior, C. R. Díaz, C. Marques, M. J. Pontes, and A. Frizera, "Multiplexing technique for quasi-distributed sensors arrays in polymer optical fiber intensity variation-based sensors," *Opt. Laser Technol.*, vol. 111, pp. 81–88, Apr. 2019.
[10] W. Zhang *et al.*, "Analysis of long-distance distributed optical fiber sensing technology," *Electron. Technol.*, vol. 51, no. 2, pp. 8–9, 2022.
[11] X. Yusheng, "Application of optical fiber sensing technology in safety monitoring of high-speed railway infrastructure," *Railway Construct.*, vol. 9, pp. 143–147, 2016.
[12] P. Lu *et al.*, "Distributed optical fiber sensing: Review and perspective," *Appl. Phys. Rev.*, vol. 6, no. 4, Sep. 2019, Art. no. 041302.
[13] A. Barrias, J. Casas, and S. Villalba, "A review of distributed optical fiber sensors for civil engineering applications," *Sensors*, vol. 16, no. 5, p. 748, May 2016.
[14] Z. Qin, T. Zhu, L. Chen, and X. Bao, "High sensitivity distributed vibration sensor based on polarization-maintaining configurations of phase-OTDR," *IEEE Photon. Technol. Lett.*, vol. 23, no. 15, pp. 1091–1093, Aug. 1, 2011.
[15] Z. Pan, K. Liang, Q. Ye, H. Cai, R. Qu, and Z. Fang, "Phase-sensitive OTDR system based on digital coherent detection," in *Proc. Asia Commun. Photon. Conf. Exhib. (ACP)*, Nov. 2011, pp. 1–6.
[16] X. Zhang *et al.*, "A high performance distributed optical fiber sensor based on Φ-OTDR for dynamic strain measurement," *IEEE Photon. J.*, vol. 9, no. 3, pp. 1–12, Jun. 2017.
[17] Z. Z. Wang *et al.*, "Generation mechanism and suppression method of optical background noise in phase-sensitive optical time-domain reflection sensing system," *J. Phys.*, vol. 66, no. 7, pp. 87–100, 2017.
[18] Y. Y. Shao *et al.*, "Distributed vibration sensor with laser phase-noise immunity by phase-extraction Φ-OTDR," *Photonic Sensors*, vol. 9, no. 3, pp. 223–229, 2019.
[19] Y. Lu, T. Zhu, L. Chen, and X. Bao, "Distributed vibration sensor based on coherent detection of phase-OTDR," *J. Lightw. Technol.*, vol. 28, no. 22, pp. 3243–3249, Nov. 15, 2010.
[20] T. Zhu *et al.*, "Enhancement of SNR and spatial resolution in Φ-OTDR system by using two-dimensional edge detection method," *J. Lightw. Technol.*, vol. 31, no. 17, pp. 2851–2856, Sep. 16, 2013.
[21] H. Yue *et al.*, "Simultaneous and signal-to-noise ratio enhancement extraction of vibration location and frequency information in phase-sensitive optical time domain reflectometry distributed sensing system," *Opt. Eng.*, vol. 54, no. 4, Apr. 2015, Art. no. 047101.
[22] Y. Muanenda *et al.*, "Dynamic phase extraction in a modulated double-pulse Φ-OTDR sensor using a stable homodyne demodulation in direct detection," *Opt. Exp.*, vol. 26, no. 2, pp. 687–701, 2018.
[23] F. Jiang *et al.*, "High-fidelity acoustic signal enhancement for phase-OTDR using supervised learning," *Opt. Exp.*, vol. 29, no. 21, pp. 33467–33480, 2021.
[24] Q. Ma, X. Gao, Y. Gao, X. Zhang, and Z. Zhong, "A study on noise reduction of Φ-OTDR system based on VSS-NLMS algorithm," *IEEE Sensors J.*, vol. 21, no. 6, pp. 7648–7656, Mar. 2021.
[25] Y. C. Eldar, *Sampling Theory: Beyond Bandlimited Systems*. Cambridge, U.K.: Cambridge Univ. Press, 2015.
[26] S. A. Mallat, *Wavelet Tour of Signal Processing*. Amsterdam, The Netherlands: Elsevier, 1999.
[27] M. Elad, *Sparse and Redundant Representations: From Theory to Applications in Signal and Image Processing*. New York, NY, USA: Springer, 2010.
[28] R. G. Baraniuk, "Compressive sensing [lecture notes]," *IEEE Signal Process. Mag.*, vol. 24, no. 4, pp. 118–121, Jul. 2007.
[29] E. J. Candès and T. Tao, "Decoding by linear programming," *IEEE Trans. Inf. Theory*, vol. 51, no. 12, pp. 4203–4215, Dec. 2005.
[30] E. J. Candès, "The restricted isometry property and its implications for compressed sensing," *Comp. Rendus Mathematique*, vol. 346, nos. 9–10, pp. 589–592, Feb. 2008.

**Xu Gao** received the bachelor's degree from Jilin University (JLU), China, in 2009, and the Ph.D. degree from the Changchun Institute of Optics, Fine Mechanics and Physics (CIOMP), China, in 2014. She is currently an Associate Professor at the Changchun University of Science and Technology (CUST). Her current research interests include photoelectric displacement precision measurement technology and optical fiber sensor.

**Wenhao Hu** received the bachelor's degree from Dalian Maritime University. He is pursuing the master's degree with the Changchun University of Science and Technology. His main research interest content is optical fiber sensors.

**Zhijiang Dou** received the bachelor's degree from the Changchun University of Science and Technology. He is pursuing the master's degree with the Harbin Institute of Science and Technology. His main research interests lie in photoelectric signal demodulation and processing.

**Kaiwei Li** received the B.E. degree in mechanical engineering from Jilin University, Changchun, China, in 2009, and the Ph.D. degree in mechanical engineering from the Changchun Institute of Optics, Fine Mechanics and Physics, Chinese Academy of Sciences, Changchun, in 2014. In 2015, he joined the Centre for Optical Fibre Technology, Nanyang Technological University, Singapore, as a Research Fellow. In 2019, he joined the Institute of Photonics Technology, Jinan University, Guangzhou, China. In 2022, he joined the Key Laboratory of Bionic Engineering, Ministry of Education, Jilin University. His research interests include fiber-optic sensors and specialty optical fibers.

**Xuepeng Gong** was with the Changchun Institute of Optics, Fine Mechanics and Physics, Chinese Academy of Sciences, Changchun, China. He is a Professor and a Doctoral Supervisor at the Changchun Institute of Optics, Fine Mechanics and Physics, Chinese Academy of Sciences. His current research interests include development of beamline equipments of synchrotron radiation facility and free electron laser facility, and research on EUV multilayer film life.